New methods for onset detection of acoustic emission signals

Daniel Gagar[1], **Fangliang Bai**[2], **Yifan Zhao**[1], **Peter Foote**[1]

[1] School of Aerospace, Transport and Manufacturing, Cranfield University, Bedfordshire, MK43 0AL, UK

Keywords: Onset detection, acoustic emission, signal-to-noise ratio, damage location

Abstract

Acoustic Emission (AE) monitoring can be used to detect the presence of damage as well as determine its location in Structural Health Monitoring (SHM) applications. The onset time of AE signals detected at different sensors in an array is used to determine their relative time difference of arrival which is essential in performing localisation of the signals' originating source.Typically, this is done using a fixed threshold which is particularly prone to errors when not set to optimal values. This paper presents three new methods for determining the onset of AE signals without the need for a predetermined threshold. The performance of the techniques in terms of location accuracy is evaluated using AE signals generated during fatigue crack growth and compared to the established fixed threshold method. It was found that the mean absolute error in performing 1D location using the new methods was between 11.6 to 14.3 mm compared to a range of 19.3 to 37.2 mm for the conventional Fixed Threshold method at different threshold levels.

1. INTRODUCTION

Acoustic Emission (AE) monitoring is a type of Structural Health Monitoring (SHM) technique which can be used to perform continuous assessment of structural integrity via permanently installed sensors. AE stress waves are dynamically excited as a result of instantaneous mechanical loading from accidental impacts or growing defects such as fatigue cracks in metals and delamination in composites. The location of damage can be determined using the expression in Equation (1). The required inputs are measurements of signal Time Difference of Arrival (TDOA) obtained from different sensors in an array, as well as the propagating wave velocity and sensor coordinates. Errors in specifying each of these parameters will contribute to the errors observed in accurately locating the source of the signals detected. This paper if focused on the potential errors associated with TDOA measurements as a function of AE signal onset detection.

$$(x_i - x_o)^2 + (y_i - y_o)^2 = (V_g \cdot \Delta t)^2 \tag{1}$$

Where,
(x_o, y_o) and (x_i, y_i) are the coordinates of source and sensors for i = 1,...n,
Δt is the time difference of arrival of signal between different sensors,
V_g is the propagating wave velocity.

Onset detection of AE signals is most commonly performed using the fixed threshold method, where the first instance of signal amplitude exceeding a specified valued indicates the onset of the signal [1, 2]. The main drawback of this technique is the selection of an appropriate threshold value for signal detection with respect to the background noise; a value too low might prematurely trigger onset detection and a value too high would likely introduce a lag in onset detection. This challenge is significantly compounded with low signal to noise ratio. Other alternative methods have been developed in both the time and time-frequency domains, however they often tend to either depend on some form of threshold predetermined by trial and error, or are inherently unstable. In this paper, three new methods for AE signal onset detection are presented and their performance evaluated in terms of accuracy.

2. METHODOLOGY

Three new methods have been developed to perform AE signal onset detection and TDOA measurements based on analyses in the time domain and the time-frequency domain.

2.1 Time-varying Correlation Method

This method is based on cross-correlation and the surrogate significance test in the time domain to automatically determine the onset of AE signals. It is a variant of the traditional cross-correlation, performed using a sliding window centred at position t and with duration h. Consider two signals U = *u(1), u(2),...u(n)* and V = *v(1), v(2),...v(n)*, the cross-correlation between these two signals can be calculated using the expression in Equation (2).

$$r_{uv}(d) = \frac{\sum_{i=1}^{n}(u(i)-\overline{U})(v(i-d)-\overline{V})}{\sqrt{\sum_{i=1}^{n}(u(i)-\overline{U})^2}\sqrt{\sum_{i=1}^{n}(v(i)-\overline{V})^2}} \tag{2}$$

Where $\overline{U}$ and $\overline{V}$ are the means of the signals U and V respectively, n is the number of samples, and d = *0,1,2,...n-1* is the time delay. The magnitude of the cross-correlation function $r_{uv}(d)$ represents the level of similarity between these two signals with the time shift and the maximum value k, as expressed in Equation 6, indicates the time when both signals are aligned with the most similar characteristics.

$$k = \underset{d}{\operatorname{argmax}}(r_{uv}(d)) \tag{3}$$

The level of correlation at time t is denoted by *s(t)* and expressed in Equations (4). The maximum of the function *s(t)* is similarly indicative of the time when both signals are aligned with the most similar characteristics. Figure 2 shows the cross-correlation series for AE signals recorded by a pair of sensors, as shown in Figure 1, with different distances from the AE event source location.

$$s(t) = \underset{d}{\operatorname{argmax}}(r_{uv}(t,d)) \tag{4}$$

Where,

$$r_{uv}(t,d) = \frac{\sum_{i=t-h/2}^{t+h/2}(u(i)-\overline{U})(v(i-d)-\overline{V})}{\sqrt{\sum_{i=t-h/2}^{t+h/2}(u(i)-\overline{U})^2}\sqrt{\sum_{i=t-h/2}^{t+h/2}(v(i)-\overline{V})^2}} \tag{5}$$

The onset time of a signal corresponds to the point where there is a significant step change in the series of the time-varying correlation function *s(t)*. This can be automatically detected using the Surrogate significance test [3–5]. This is a statistical technique used to detect non-linearity in a time series. Assuming the signal U is related to the signal V, this sort of dependence is lost when V is re-ordered randomly. The order of the data in V is randomised by a shuffle procedure that saves the distribution properties of the signal V, but destroys the temporal relationship between U and V. In this paper, an Amplitude Adjusted Fourier Transform (AAFT) randomization surrogate technique [4] is applied. This is done by performing a Fourier transform of the signal V using its randomised phase whilst preserving the amplitude in the process. The surrogate version of the original signal is generated by applying the inverse Fourier transform and referred to as the surrogate signal. The time-varying correlation between the signal U and the surrogate data is then calculated. This procedure is repeated 100 times to achieve statistical significance as suggested in reference [6]. The correlation series for the surrogate signal, denoted by $\tau(t)$, is defined as the 95% quantile of 100 tests for each time step t. Searching from the time when *s(t)* reaches the maximum toward the left direction, the TOA for the signal U is represented by the first time when *s(t)* is below $\tau(t)$. As shown in Figure 2(a), the blue plot illustrates *s(t)* and red curve plots $\tau(t)$, and the TOA is determined as $247\mu s$.

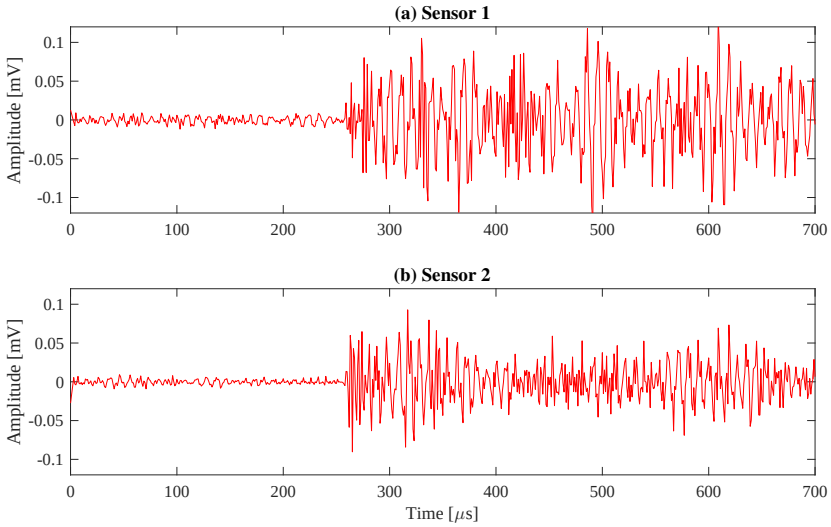

Figure 1 : AE signals from the same event recorded by a pair of sensors at different locations

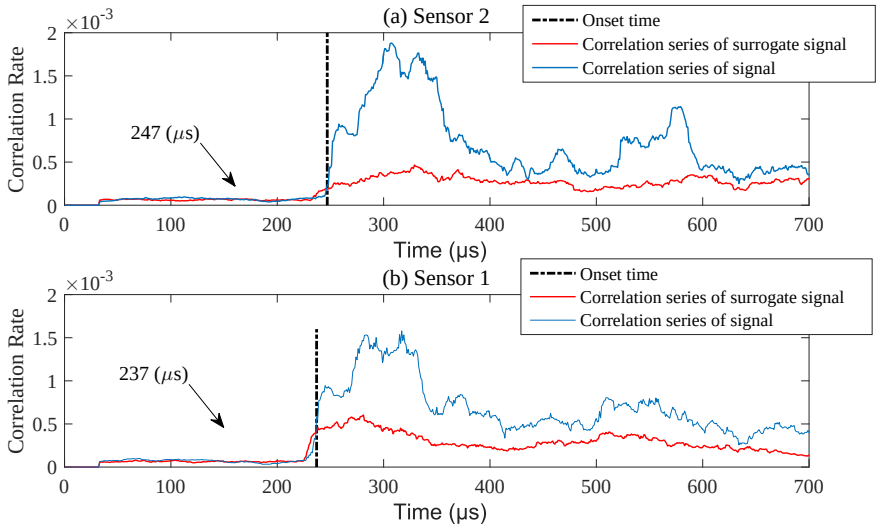

Figure 2 : AE signal onset detection using the Time-varying correlation method for (a) sensor 1 and (b) sensor 2. The blue line indicates the correlation series of the raw signals and red line is for correlation series of surrogate signals

By swapping the signal U for V, the TOA for the signal V can be detected, as illustrated by Figure 2(b). The value of TDOA is finally calculated using Equation (6).

$$TDOA(U,V) = |TOA_U - TOA_V| \tag{6}$$

2.2 CWT-based Correlation Method

This method is based on cross-correlation and the surrogate significance test as described in the Section 2.1, however the analysis is performed in the time-frequency domain to automatically determine the onset of AE signals. Continuous wavelet transform (CWT) is used to produce a spectrum of time-frequency according to the relationship between the scale and the frequency. Considering a signal *u(t)*, the coefficient of its CWT at a scale $a(a > 0, a \in \mathbb{R})$ and translational value $b \in \mathbb{R}$ is expressed as:

$$c(a,b;x(t),\phi(t)) = \int_{-\infty}^{\infty} x(t)\frac{1}{\sqrt{a}}\phi * \left(\frac{t-b}{a}\right) dt \tag{7}$$

Where $\phi(t)$ is a continuous function in both time and frequency domains called the mother wavelet and the $*$ represents the operation of complex conjugate. Figure 3 shows the CWT spectrum of the pair of AE signals shown in Figure 1.

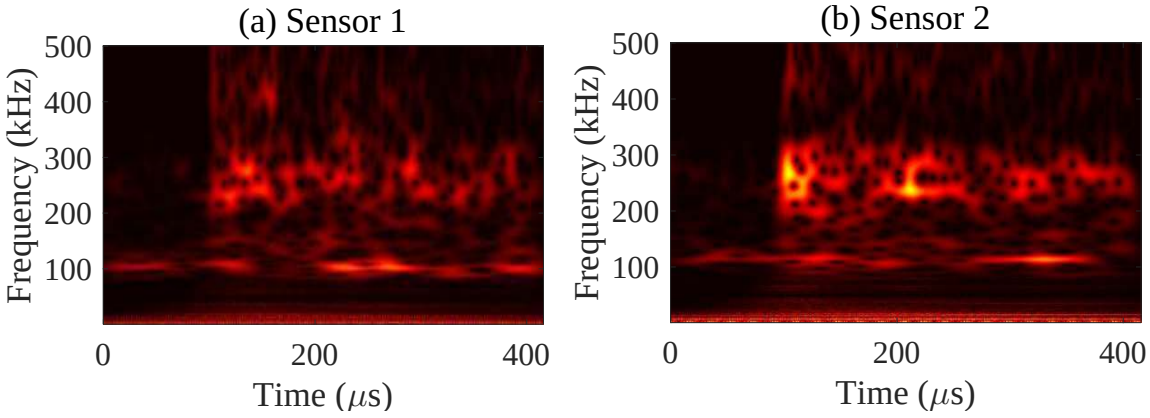

Figure 3 : CWT spectrum for AE signals recorded by a pair of sensor with different distances from the AE event location

The CWT-based correlation method basically involves performing cross-correlation of the CWT coefficients for consecutive time samples of a signal. The frequency distribution of an AE signal at any time before signal onset is known to be pseudo-random and, therefore, the correlation between CWT coefficients for two consecutive time samples in this period can be expected to be low. In contrast, the frequency distribution of an AE signal at any time after the signal onset is relatively coherent due to its inherent periodicity, which also suggests that the correlation between CWT coefficients for two consecutive time samples in this period is high. The blue plots in Figure 4 show the cross-correlation series of the CWT coefficients for the AE signals shown in Figure 1.

The onset of a signal corresponds to the point where there is a significant step change in the cross-correlation of the CWT coefficients. The Surrogate significance test is also applied, as previously described in Section 2.1, to automatically determine the onset time of the signals. Figure 4 shows the cross-correlation series of the CWT coefficients for the surrogate signals, illustrated by the red plots.

The CWT-based correlation method can be summarised as the following steps.

1. Calculate the time-frequency response for the signal U based on CWT.
2. Calculate the time-varying correlation between two consecutive columns of CWT coefficients, denoted as $w_U(t)$.
3. Generate the surrogate signal and apply step 1-2.
4. Repeat step 3 for 100 times and the 95% quantile of all tests at each time is chosen as the surrogate threshold, denoted as $\tau_U(t)$.
5. Searching from the time when $w_U(t)$ reaches the maximum toward the left direction, the TOA for the signal is indicated by the first time when $w_U(t)$ is below $\tau_U(t)$.
6. Repeat step 1-5 for the next signal V.
7. Calculate the TDOA based on the function (6).

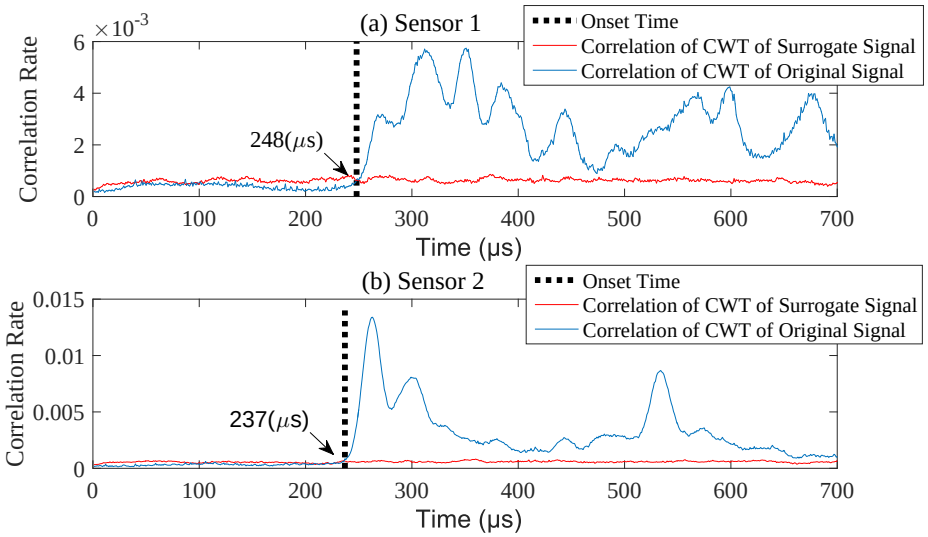

Figure 4 : AE signal onset detection using the CWT-based correlation method for (a) sensor 1 and (b) sensor 2. The blue line indicates the correlation series of the raw signal and red line is for correlation series of surrogate signal

2.3 CWT-based Binary Map

This method utilises the CWT coefficients of an AE signals time-frequency response to construct a greyscale image, with the magnitude of each component representing the intensity of a pixel. The presence of noise in the image is minimised by applying a Median filter [7]. This is a nonlinear digital filtering technique where the intensity of each pixel is replaced by the median intensity of the neighbouring pixels.

The onset of the signal is determined by performing an image segmentation to create clear contrast in its features, from which the leading edge can be identified. This involves converting the greyscale image to a binary image where each pixel is assigned a value of 0 or 1 depending on whether its intensity exceeds or falls below an optimal level. The Otsu's method is used to automatically determine the optimal intensity level at which the intra-class variance is minimum and the inter-class variance is maximum [8].

The onset time of an AE signal can therefore be determined by finding the leftmost non-zero pixel in the binary image. The effectiveness of the method may be improved by applying in a band of frequency which can be specified if the frequency characteristics of the AE signal are known. Figure 5 shows an example of a binary map image generated for a pair of AE signals with indications of their respective onset times.

The CWT based binary map method can be summarised as:

1. Calculate the time-frequency response for the signal U based on CWT.
2. Normalise the power spectrum to generate a grey-scale image.
3. Reduce noise using a Median filter.
4. Generate a binary map using the Otsu's method.
5. Detect the earliest non-zero pixel to represent the TOA for the signal.
6. Repeat step 1-5 for the next signal V.
7. Calculate the TDOA.

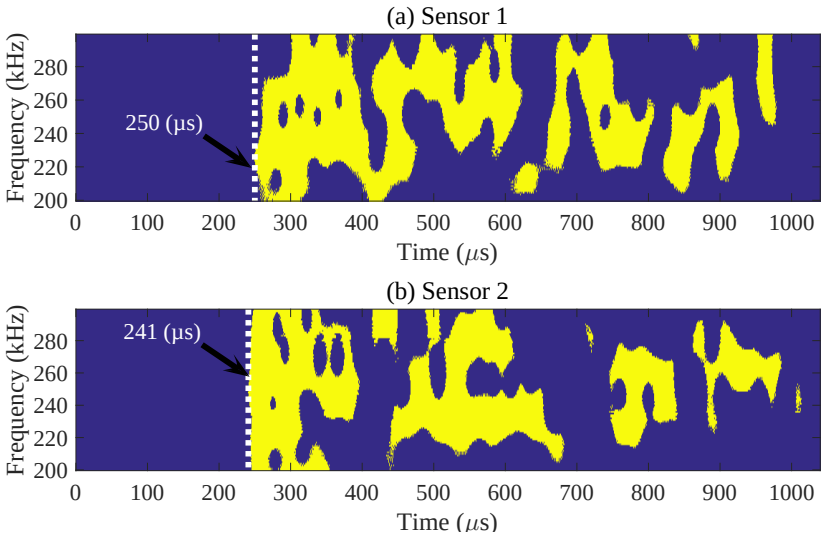

Figure 5 : AE signal onset detection using the CWT-based binary map method for (a) sensor 1 and (b) sensor 2

3. EXPERIMENTS

An experiment in which AE signals were generated by growing cracks in a metal specimen undergoing mechanical fatigue was performed in order to evaluate and compare the three TDOA measurement methods described above. A fatigue crack growth test was performed on a Single Edge Notch (SEN) 2014 T6 aluminium sample with thickness of 2 mm as illustrated in Figure 6. The sample was subjected to constant amplitude fatigue loading with stress range of 52 MPa, stress range of 0.1 and frequency of 2 Hz.

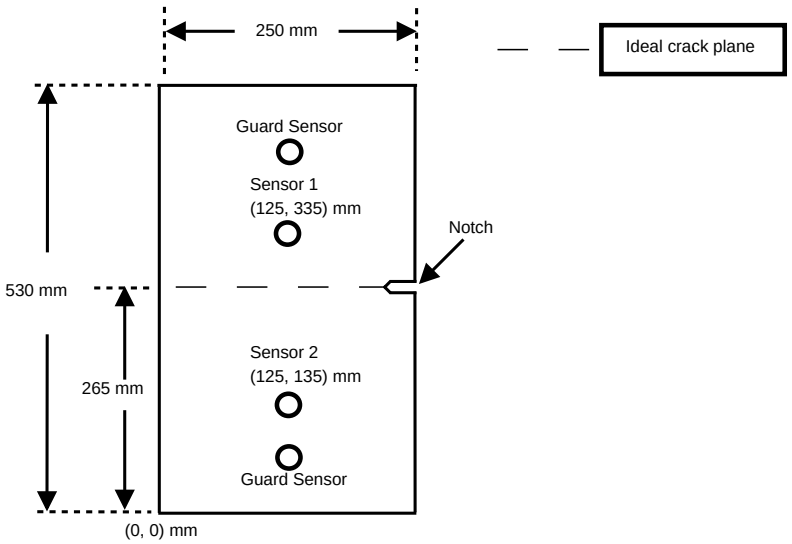

Figure 6 : Test sample geometry and layout of AE sensors

A multi-channel Physical Acoustics AE system (PCI-2) was used to record AE signals using broad-band piezoelectric sensors (WDI), at positions as indicated in Figure 6, with sampling rate of 1 MS/s and a pre-amplifiers with band-pass frequency filters in the range of 20 - 1200 kHz. The fixed detection threshold was set at 45 dB and the pre-amplifier gain for each channel was set to 40 dB. Exclusive monitoring of AE signals generated from the fatigue crack was achieved by implementing a spatial filter set

to reject spurious signals generated from the test machine grips using guard sensors, illustrated in Figure 6.

4. RESULTS

AE signals were recorded throughout the test, from fatigue crack initiation until final failure, and a total of 111 AE events were randomly selected for further analysis. Measurements of the TDOA for all the AE events were determined using each of the new methods previously described in Section 2, alongside the already established fixed threshold method. Theoretical values for the propagating wave velocity were assumed. The dispersion relation for the fundamental wave modes is shown in Figure 7, obtained using Wavescope [9]. The average wave group velocity for frequencies up to 400 kHz is 5305.5 m/s $\pm$ 81.5.

The results for the distribution of the range of location estimates are shown in Figure 8 for the various threshold-independent methods and Figure 9 for the Fixed Threshold method at different threshold levels; the origin (at 0 mm) represents the true location of the fatigue crack plane. It can be seen that although the distributions are typically multi-modal, the most dominant mode is centred in the vicinity of the crack location for the case of the location estimates obtained using the Binary Map and the CWT-based correlation methods. In contrast, the dominant mode for the Fixed Threshold method at all the threshold levels is about 30 mm away from the actual crack location.

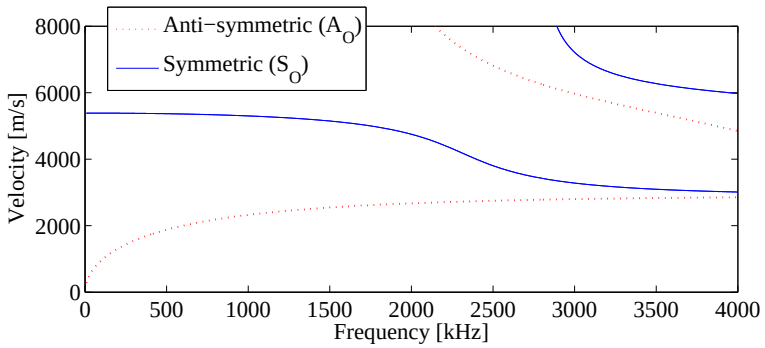

Figure 7 : Dispersion relation for the fundamental Lamb wave modes in 2mm thick 2014-T6 Aluminium

The Mean Absolute Error (MAE) and corresponding standard deviations (σ) were calculated for each of the distributions as a measure of location accuracy and precision. For the threshold-independent methods, it was observed that in terms of location accuracy the Binary Map method produced the least mean absolute location error of 11.6 mm and the CWT-based Correlation method produced the largest mean absolute location error of 14.3 mm as shown in Table 1. In the case of the Fixed Threshold method, it can also be seen that the MAE consistently increases with increased threshold level.

In terms of location precision, the Time-varying Correlation method produced the least spread in the distribution with a standard deviation of 16.6. The Fixed Threshold method also showed a trend of consistently increasing standard deviation with increased threshold level.

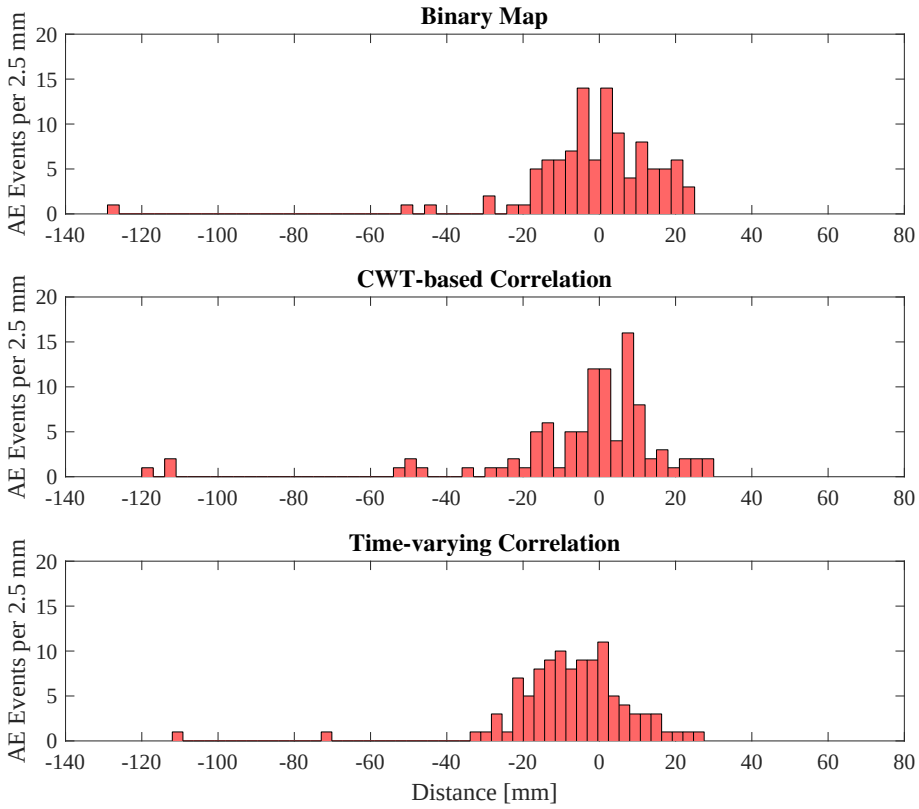

Figure 8 : Distribution of 1-Dimensional location estimates using various threshold-independent methods

Table 1 : Comparison of accuracy and precision of the distribution of errors in AE event location estimates obtained with the various methods

		Accuracy	Precision
		MAE [mm]	Standard Deviation [mm]
Binary Map		11.6	18.2
CWT-based Correlation		14.3	16.6
Time-varying Correlation		11.9	25.0
Fixed threshold	40 dB	19.3	22.2
	45 dB	25.2	38.3
	50 dB	37.2	49.1

5. DISCUSSION

The results have shown that for representative AE signals with a nominal SNR (11.4464 dB) the three new threshold-independent methods yielded improved 1D location accuracy compared with the established amplitude threshold method. The threshold-independent techniques produced Mean Absolute Errors in the range 11.6 to 14.3 mm. In contrast, the amplitude threshold method produced errors in the range 19.3 to 37.2 mm at different threshold levels. From this it can be concluded that some improvement in accuracy of location of AE events could be gained using the proposed threshold-independent methods with the binary map technique producing the lowest error for these tests.

The robustness of these techniques to decreasing SNR values however also needs to be evaluated. This is significant for applications using AE detection as a form of structural heath monitoring where

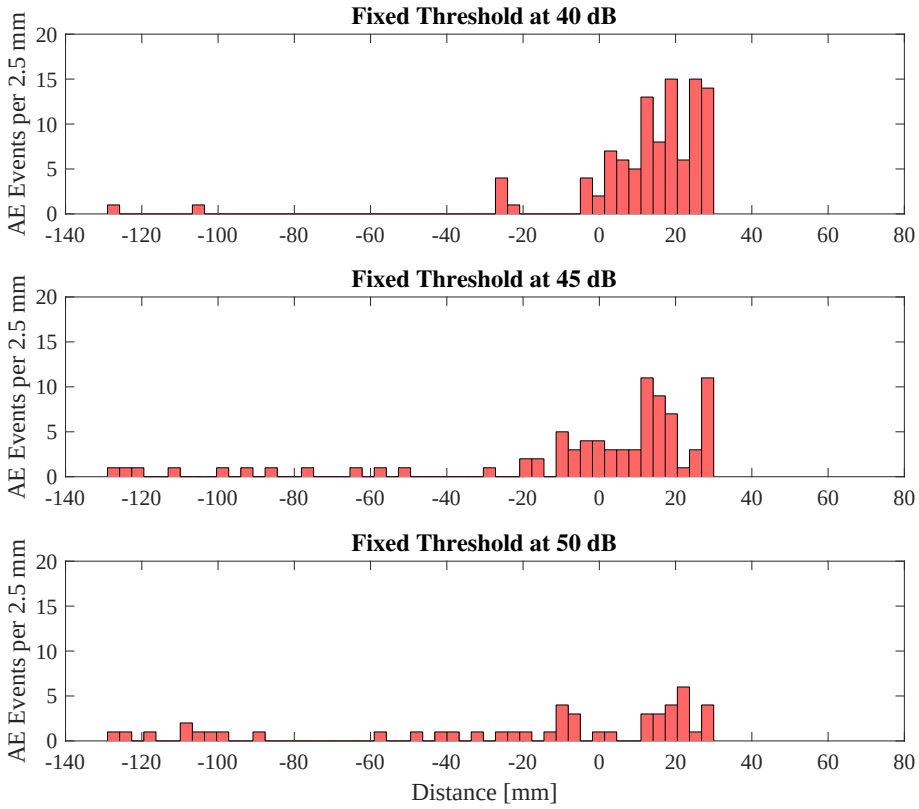

Figure 9 : Distribution of 1-Dimensional location estimates using the Fixed Threshold method at different threshold levels

sensors can experience ageing or degradation during their lifetimes. In such scenarios it is feasible that sensor SNR can degrade, which will pose a challenge in the accuracy of TDOA measurements and consequently the accuracy of damage location. This will form the basis of future work on this subject.

6. CONCLUSIONS

1. Three new threshold-independent techniques for performing AE signal onset detection techniques have been developed in the time and time-frequency domains
2. The 1D location accuracy of these techniques was within 7.1% of the monitored region compared to a range of 9.7 - 18.6% for the conventional Fixed Threshold method at different threshold levels.
3. The 1D location precision of these techniques was also demonstrated to be an improvement of the conventional Fixed Threshold method.

ACKNOWLEDGEMENT

Enquiries for access to the data referred to in this paper should be directed to research-data@cranfield.ac.uk.

REFERENCES

[1] M J Eaton, R Pullin, and K M Holford. Towards improved damage location using acoustic emission. *Proceedings of the Institution of Mechanical Engineers, Part C: Journal of Mechanical Engineering Science*,

226(9):2141–2153, 2012.

[2] P Sedlak, Y Hirose, and M Enoki. Acoustic emission localization in thin multi-layer plates using first-arrival determination. *Mechanical Systems and Signal Processing*, 36(2):636–649, 2013.

[3] D Prichard and J Theiler. Generating surrogate data for time series with several simultaneously measured variables. *Physical Review Letters*, 73(7):951–954, 1994.

[4] J Theiler, S Eubank, A Longtin, B Galdrikian, and J Doyne Farmer. Testing for nonlinearity in time series: the method of surrogate data. *Physica D: Nonlinear Phenomena*, 58(1-4):77–94, 1992.

[5] Yifan Zhao, Steve A. Billings, and Hualiang Wei. Tracking time-varying causality and directionality of information flow using an error reduction ratio test with applications to electroencephalography data. *Physical Review E*, 86:051919, 2012.

[6] Thomas Schreiber and Andreas Schmitz. Surrogate time series. *Physica D: Nonlinear Phenomena*, 142(34):346 – 382, 2000.

[7] T S Huang, G J Yang, and G Y Tang. A Fast Two-Dimensional Median Filtering Algorithm. *IEEE Transactions on Acoustics, Speech, and Signal Processing*, 27(1):13–18, 1979.

[8] Nobuyuki Otsu. Threshold selection method from gray-level histograms. *IEEE Trans Syst Man Cybern*, SMC-9(1):62–66, 1979.

[9] Laboratory for Active Materials (LAMSS) and Smart Structures. WAVESCOPE: Dispersion curves, Group velocities and Tuning for metallic structures.